

Influences of Al doping on the electronic structure of Mg(0001) and dissociation property of H₂

Yanfang Li,^{1,2} Yu Yang,² Yinghui Wei,¹ and Ping Zhang^{2,*}

¹*College of Materials Science and Engineering,
Taiyuan University of Technology, Taiyuan 030024, People's Republic of China*

²*LCP, Institute of Applied Physics and Computational Mathematics,
P.O. Box 8009, Beijing 100088, People's Republic of China*

(Dated: November 21, 2018)

Abstract

By using the density functional theory method, we systematically study the influences of the doping of an Al atom on the electronic structures of the Mg(0001) surface and dissociation behaviors of H₂ molecules. We find that for the Al-doped surfaces, the surface relaxation around the doping layer changes from expansion of a clean Mg(0001) surface to contraction, due to the redistribution of electrons. After doping, the work function is enlarged, and the electronic states around the Fermi energy have a major distribution around the doping layer. For the dissociation of H₂ molecules, we find that the energy barrier is enlarged for the doped surfaces. Especially, when the Al atom is doped at the first layer, the energy barrier is enlarged by 0.30 eV. For different doping lengths, however, the dissociation energy barrier decreases slowly to the value on a clean Mg(0001) surface when the doping layer is far away from the top surface. Our results well describe the electronic changes after Al-doping for the Mg(0001) surface, and reveal some possible mechanisms for improving the resistance to corrosion of the Mg(0001) surface by doping of Al atoms.

PACS numbers: 73.90.+f, 73.20.Hb, 82.20.Kh.

*Corresponding author. E-mail address: zhang_ping@iapcm.ac.cn

I. INTRODUCTION

Since hydrogen is one of the best clean fuels in the future, looking for an ideal storage material has become an important task for experimental and theoretical researchers. Among all the candidates, magnesium (Mg) based materials are widely concerned because they are relatively inexpensive and can hold a high weight percentage of hydrogen [1, 2]. So the interaction between hydrogen and Mg has been extensively studied [3–8]. The main disadvantage that prevents the vast applications of Mg for hydrogen storage lies in that the corresponding hydrogenation and dehydrogenation temperatures are large [1, 2]. Recently, it is found that the aluminum (Al) doped MgAl thin films have much lower hydrogenation temperatures than pure Mg films [1, 9]. However, the specific reason for the improvement as well as the influence of Al doping on the electronic properties of Mg films, remains unclear. So, in order to advance the searches for ideal hydrogen storage materials and applications of hydrogen fuels, it become quite important to make clear the influence of Al doping on the electronic structure of Mg and the the interaction between hydrogen and Mg.

Apart from the potential usages in hydrogen storage, MgAl alloys are also important industrial materials used in aerospace applications [10]. It is always believed that the Al doping makes Mg more resistant to being corrupted by air. So lots of efforts have been applied to upgrade the manufacturing techniques to dope Al in Mg materials, and now the technology has become quite mature. Studying the interactions between small molecules and Al-doped Mg surfaces can give us critical information about the mechanisms for Al doping to improve the resistance of Mg to corruption, and thus are very meaningful and necessary. Based on this background and the requirements of hydrogen storage materials, we here perform first principles calculations to systematically study the influence of Al doping on the electronic properties of the Mg(0001) surface and the adsorption behavior of hydrogen molecules.

Previous studies have revealed that the Mg(0001) surface has both considerable *s* and *p* electronic states distributing around the Fermi energy, because of the *sp* hybridizations [11]. Here we further find that after doping of an Al atom, the electronic structures around the Fermi energy mainly distribute around the doping layer. For the dissociation of hydrogen molecules on the clean Mg(0001) surface, it has been found that the most energetically favored site is the surface bridge site [6–8, 12], with the corresponding minimum energy

barrier of 0.85 eV [12]. Through our present first-principles calculations, we find that Al-doping will not change the most energetically favored dissociation channel. However, the minimum energy barrier for dissociation of hydrogen is critically dependent on the doping depth of Al, and the values are all larger than that on the clean Mg(0001) surface. The rest of this paper is organized as follows: In Sec. II, we describe our first-principles calculation method and the models used in this paper. In Sec. III, we present in detail our calculated results, including the comparisons of the electronic structures of the Mg(0001) surface before and after Al doping, and the dissociation of hydrogen molecules on the Al-doped Mg(0001) surface. At last, the conclusion is given in Sec. IV.

II. CALCULATIONAL METHODS

Our calculations are performed within density functional theory (DFT) using the Vienna *ab-initio* simulation package (VASP) [13]. The PW91 [14] generalized gradient approximation and the projector-augmented wave potential [15] are employed to describe the exchange-correlation energy and the electron-ion interaction, respectively. The cutoff energy for the plane wave expansion is set to 250 eV, which is large enough to make the calculational error of the adsorption energy below 0.01 eV. The clean and Al-doped Mg(0001) surface are modeled by a slab composing of five atomic layers and a vacuum region of 20 Å. The 2×2 supercell in which each monolayer contains four Mg atoms are adopted in the study of the H₂ adsorption. Our test calculations have shown that the 2×2 supercell is sufficiently large to avoid the interaction between adjacent hydrogen molecules. Integration over the Brillouin zone is done using the Monkhorst-Pack scheme [16] with $11 \times 11 \times 1$ grid points. A Fermi broadening [17] of 0.1 eV is chosen to smear the occupation of the bands around the Fermi energy (E_f) by a finite- T Fermi function and extrapolating to $T = 0$ K. During geometry optimizations, the bottom layer of the clean and Al-doped Mg(0001) surface is fixed while other Mg and Al atoms are free to relax until the forces on them are less than 0.01 eV/Å. The calculation of the potential energy surface for molecular H₂ is interpolated to 209 points with different bond length ($d_{\text{H-H}}$) and height (h_{H_2}) of H₂ at each surface site. The calculated lattice constant of bulk Mg (a , c) and the bond length of a free H₂ molecule are 3.21 Å, 5.15 Å and 0.75 Å, respectively, in good agreement with the experimental values of 3.21 Å, 5.20 Å [18, 19] and 0.74 Å [20].

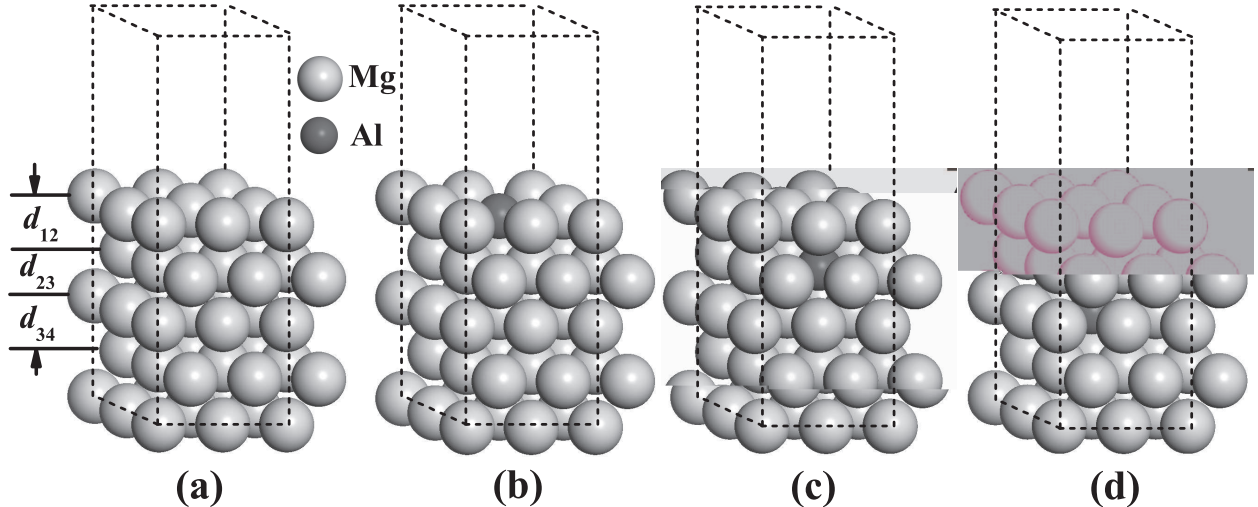


FIG. 1: (Color online). Atomic configurations of the Mg(0001) (a), MgAl1 (b), MgAl2 (c), and MgAl3 (d) surfaces, with the corresponding supercells depicted in dashed lines. Mg and Al atoms are shown in grey and dark grey balls.

III. RESULTS AND DISCUSSION

As shown in Fig. 1, we have employed 3 different doping depths for Al in the Mg(0001) surface, with the Al atom respectively in the first (MgAl1), second (MgAl2) and third monolayer (MgAl3). For the clean Mg(0001) surface, our calculations reveal that the distances between the three topmost atomic layers are expanded from their bulk values, in accordance with previous theoretical [8, 21, 22] and experimental reports [23]. It is because that due to its special surface charge redistribution, the topmost three layers of the Mg(0001) surface are negatively charged and hence repel each other. In fact, the surface expansion is a special phenomena for the Mg(0001) surface, which is not seen for other surfaces of Mg [21]. And instead of expansions, the surface relaxations of many metals show contractions [8]. The relaxation calculation for the clean Mg(0001) surface also confirms the precise of our methods.

However, after the doping of an Al atom, the surface relaxation is changed. To describe more clearly the changes, here we define the surface relaxation as

$$\Delta d_{ij} = (d_{ij} - d_0)/d_0, \quad (1)$$

where d_{ij} and d_0 are respectively the distance between the i th and j th layer of the relaxed surface, and the lattice spacing along the (0001) direction of bulk Mg. Table I summarizes

TABLE I: Surface relaxations (Δd_{12} , Δd_{23} , and Δd_{34}) and work function (Φ) of the Mg(0001), MgAl1, MgAl2, and MgAl3 surfaces.

surface	Surface relaxation			Φ (eV)
	Δd_{12} (%)	Δd_{23} (%)	Δd_{34} (%)	
Mg(0001)	+1.95	+0.55	+0.82	3.745
MgAl1	-3.00	-0.11	+0.10	3.767
MgAl2	-2.62	-2.60	+0.49	3.757
MgAl3	+0.28	-2.25	-2.12	3.757

the calculated relaxations for the clean Mg(0001), MgAl1, MgAl2, and MgAl3 surfaces. We can easily see from Table I that the results critically depend on the doping length of the Al atom. If the Al atom is doped at the first (i.e. the topmost) layer, then the distance between the first and second layers is contracted by 3.00 %. And if the Al atom is doped at the second layer, then d_{12} and d_{23} respectively decreases by 2.60 % and 2.12 %. One can see that for the layer containing the doped Al atom, the lattice spacings with its nearest Mg layers are decreased a lot from that of bulk Mg. This result is confirmed by the relaxation results of the MgAl3 surface, where d_{23} and d_{34} are decreased by 2.25 % and 2.12 %. By analyzing the atomic charges, we find that the neighboring Mg atoms always lose electrons to the doped Al atom. So the charging state of the doping layer and its neighboring Mg layers are respectively negative and positive, and the interactions between them become attracting forces. Thus the surface relaxation changes from expansion of the clean Mg(0001) surface to the contraction after Al doping.

In addition, we also calculate the work function of the doped surfaces. The calculated values are given in Table I. We can see that the doping of Al atoms enlarges the work function by 0.01~0.02 eV. It means that after doping, surface electrons become harder to escape into the vacuum, and thus the surface's reaction activity is lowered.

The band structures of the Mg(0001) and MgAl1 surfaces are calculated and shown in Fig. 2, together with their electronic density of states (DOS). By comparing Figs. 2(a) and (b), we can see that the energy bands around the Fermi energy (E_f) change a lot after Al doping. Through careful wavefunction analysis, we find that the electronic states between E_1 and E_f in Fig. 2(b) mainly distribute around the top layer. Considering that the electronic states

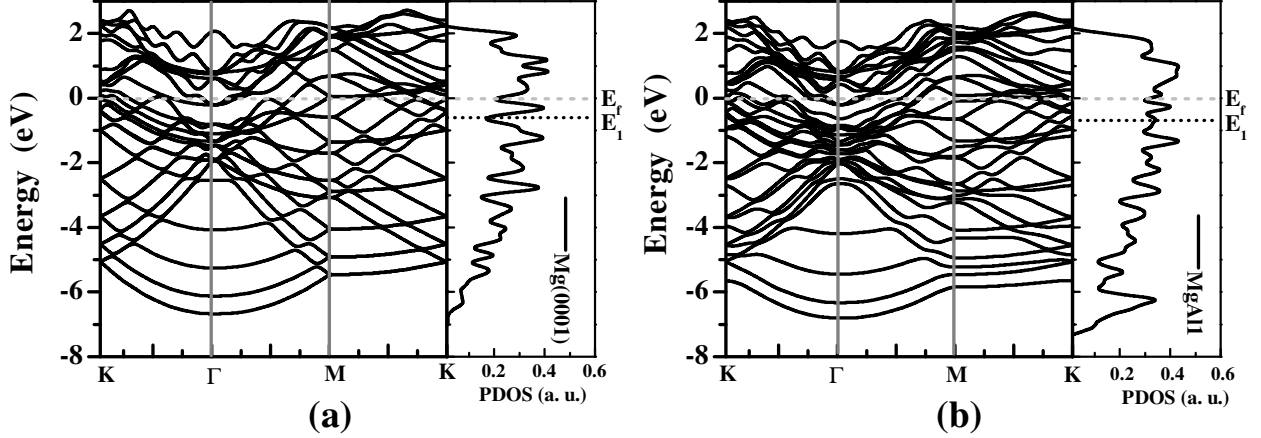


FIG. 2: (Color online). Band structures and Density of states (DOS) of the Mg(0001), MgAl1, MgAl2, and MgAl3 surfaces. The Fermi energies are set to zero.

around E_f are always more important in surface reactions, the adsorption and dissociation of small molecules on the MgAl1 surface are expected to be different from that on the clean Mg(0001) surface. As we will see, the dissociation of H_2 molecule on the MgAl1 surface does show different characters.

Moreover, we find that for different doping lengths, the result that the electronic states around E_f distribute around the doping layer still holds. As shown clearly in Fig. 3, the integral of the electronic states between E_1 and E_f for the MgAl1, MgAl2, and MgAl3 surfaces respectively have major distributions around the the first, second and third layers. Since electrons around the first layer are more easy to take part in surface reactivities, one may deduce that the influence on surface reactions is weaker for Al-doping in the second and third layers. And we will prove that it is true for the dissociation of H_2 molecules. By using the Bader topological method [24] for the MgAl1 surface, we find that the surface electron density around the first atomic layer also has a larger distribution around the Al atom, and about 3 electrons of surface Mg atoms tends to transfer to the Al atom.

After systematical studies on the electronic states of the Mg(0001), MgAl1, MgAl2, and MgAl3 surfaces. We build our model to study the adsorption of H_2 molecules. As shown in Fig. 4(a), around the doped Al atom there are four different high-symmetry sites on the surface, respectively, the top, bridge (bri), hcp and fcc hollow sites. At each site, the adsorbed H_2 molecule has three different high-symmetry orientations, respectively along the x (i.e., $[11\bar{2}0]$), y (i.e., $[\bar{1}100]$), and z (i.e., $[0001]$) directions. In the following, we will use top-

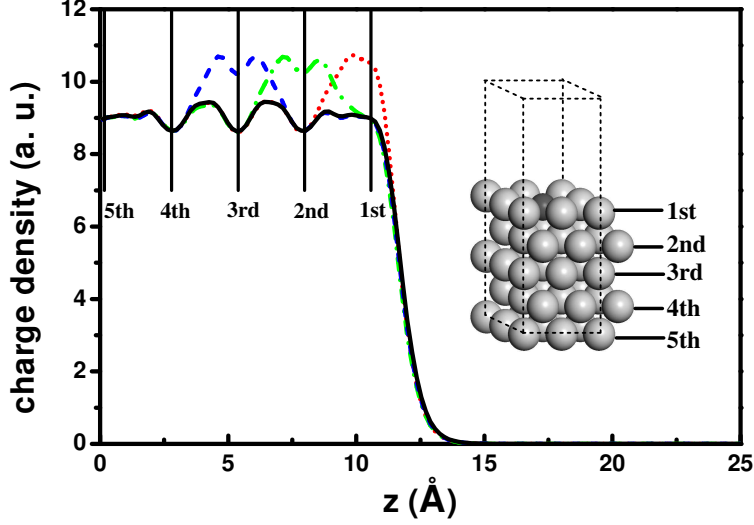


FIG. 3: (Color online). Band charge distribution around E_F of the clean and Al-incorporation Mg(0001) surface. The energy is set to $[-1.0, 0.1]$ eV.

x, y, z , $bri-x, y, z$, $hcp-x, y, z$ and $fcc-x, y, z$ respectively to represent the 12 high-symmetry channels for the approaching of H_2 . Through systematic PES calculations, we find that the dissociation energy barrier of H_2 along other low-symmetry channels is always larger than along these high-symmetry channels, similar to that observed during the dissociation of oxygen molecules on the Be(0001) surface [25].

By calculating the two-dimensional (2D) potential energy surface (PES) cuts, we find that the minimum energy path for dissociation of H_2 on the Mg(0001) surface is along the $bri-y$ channel, in accordance with previous reports [6–8]. And the corresponding energy barrier (ΔE) is 0.85 eV. After doping of an Al atom, we find that the dissociation path with the lowest energy barrier is still along the $bri-y$ channel on the MgAl1, MgAl2, and MgAl3 surfaces. The calculated energy barriers, however, are all found to be larger than that on a clean Mg(0001) surface. As a typical prototype, the PES cut for a H_2 molecule along the $bri-y$ channel on the MgAl1 surface is shown in Fig. 5. And the calculated energy barriers for the high-symmetry adsorption channels on the four surfaces are summarized in Table II, together with the bond length and height of the H_2 at the corresponding transition states. We can see from Table II that as the doping length of the Al atom is enlarged, the dissociation energy barrier approaches to the value of clean Mg(0001) surface. So the doped Al atom needs to be closer to the surface to make dissociation of H_2 harder.

Moreover, we can also see from Table II that for the $bri-y$ channel, the molecular height

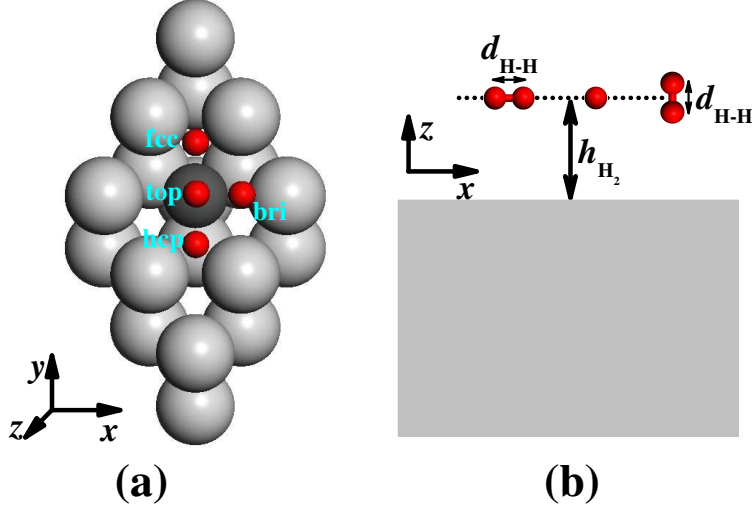


FIG. 4: (Color online). (a) The $p(2 \times 2)$ surface cell of Mg(0001) (clean or Al-doped) and four on-surface adsorption sites. (b) The sketch map showing that the molecule (with vertical or parallel orientation) is initially away from the surface with a high h_{H_2} . Mg and Al atoms are shown in grey and dark grey balls. The H_2 molecule is depicted by red balls.

for the transition state is smaller on the MgAl1 (1.04 Å) than on the clean Mg(0001) surface (1.15 Å). As we have already seen, the work function of the Mg(0001) surface is enlarged after Al-doping, and surface electrons become harder to escape into the vacuum. Since that a H_2 molecule needs two more electrons to dissociate into two hydrogen atoms, the fact that a H_2 molecule needs to be closer to the MgAl1 surface to dissociate is a chemical reflection of the change of the surface electronic states.

For the dissociation of H_2 molecules on most metal surfaces, it has been revealed that two different interactions exist, which are respectively the orthogonalizations between molecular orbitals of H_2 and electronic states of metal, and the charge transfer from metal atoms to hydrogen atoms [12, 26, 27]. As shown in Fig. 2(b), we find that the Al-doping did not change the metallic properties of the Mg(0001) surface. So such two different interactions still exist for the dissociation of H_2 on the MgAl1 surface.

Figures 6(a) and (b) respectively show the difference electron density for the adsorption system of H_2 /MgAl1 before ($h_{H_2}=2.00$ Å) and after ($h_{H_2}=0.92$ Å) the transition state along the bri- y channel, namely,

$$\Delta\rho = \rho(H_2 + MgAl1) - \rho(H_2) - \rho(MgAl1), \quad (2)$$

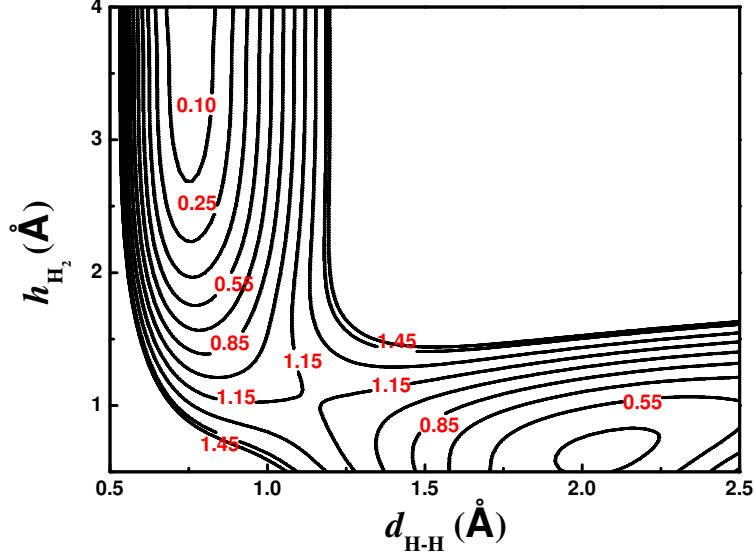


FIG. 5: (Color online). Contour plots of the two dimensional cuts of the potential energy surfaces (PESs) for dissociation of H_2 on the MgAl1 surface, as a function of the bond lengths (d_{H-H}) and the heights (h_{H_2}) along the *bri-y* adsorption channel.

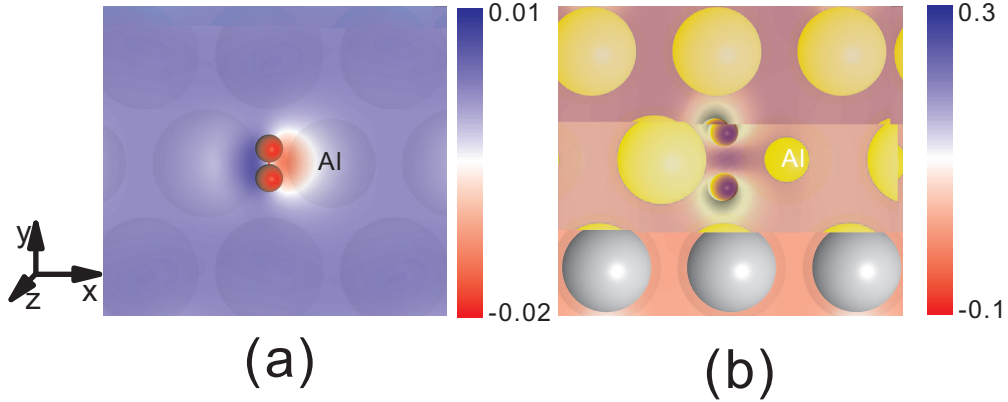


FIG. 6: (Color online). The difference electron density for the H_2 /MgAl1 system with the height of H_2 to be 2.00 (a) and 0.92 Å (b). Mg, Al, and H atoms are shown in grey, dark grey, and red balls respectively. All the values are in unit of electrons per Å³.

where $\rho(H_2 + MgAl1)$, $\rho(H_2)$ and $\rho(MgAl1)$ are respectively the electron density of the adsorption system, the H_2 molecule and the MgAl1 surface. To calculate $\Delta\rho$, the atomic positions in the last two terms in Eq. 2 have been kept at those of the first term. Through careful wavefunction analysis, we find that at the beginning of the adsorption process, the molecular orbitals of H_2 orthogonalize with electronic states of the MgAl1 surface and are

TABLE II: Energy barrier, bond length and height of the H₂ molecule at the transition states along the 12 high-symmetry adsorption channels on the Mg(0001), MgAl1, MgAl2 and MgAl3 surfaces. Energy barriers are in units of eV, while bond lengths and heights are in units of Å.

Adsorption channel	clean Mg(0001)			MgAl1			MgAl2			MgAl3		
	barrier	$d(\text{TS})$	$h(\text{TS})$	barrier	$d(\text{TS})$	$h(\text{TS})$	barrier	$d(\text{TS})$	$h(\text{TS})$	barrier	$d(\text{TS})$	$h(\text{TS})$
bri-x	1.60	1.70	1.64	1.42	1.54	1.44	1.64	1.65	1.52	1.66	1.62	1.60
bri-y	0.85	1.12	1.15	1.15	1.14	1.04	0.91	1.07	1.11	0.90	1.08	1.12
top-x	1.62	1.58	1.64	1.35	1.29	1.38	1.63	1.57	1.55	1.61	1.52	1.62
top-y	1.63	1.58	1.64	1.35	1.29	1.36	1.65	1.57	1.54	1.65	1.54	1.62
hcp-x	1.25	1.34	1.30	1.24	1.23	1.19	1.24	1.31	1.20	1.21	1.36	1.28
hcp-y	1.26	1.36	1.31	1.48	1.54	1.28	1.25	1.32	1.22	1.26	1.36	1.28
fcc-x	1.22	2.33	1.30	1.22	2.08	1.16	1.34	2.27	1.30	1.20	2.28	1.28
fcc-y	1.23	2.33	1.30	1.51	2.48	1.32	1.31	2.39	1.27	1.23	2.40	1.28

thus broadened. This orthogonalization is very similar to that has been observed during the interaction of H₂ with the Mg(0001) [12] and Al(111) [27] surfaces. As shown in Fig. 6(a), there is an electron-depletion region on top of the Al atom, which is formed because electrons around the Al atom are repelled by the H₂ bonding electrons due to the orthogonalization. In comparison, on the clean Mg(0001) surface, the electrons of Mg are repelled from the surface at the beginning of the adsorption of a H₂ molecule. We can also see from Fig. 6(b) that the H₂ molecule begins to get some electrons from the Mg and Al atoms, when it gets more closer to the MgAl1 surface.

As we have already seen, extra electrons on the MgAl1 surface trends to distribute around the Al atom. Thus during the initial stage of the adsorption of a H₂ molecule, the molecular orbitals of H₂ orthogonalize only with electronic states around the Al atom, while on the clean Mg surface, the molecular orbitals orthogonalize with electronic states around the two nearest Mg atoms. Besides, the ability to lose electrons is stronger for a Mg atom than an Al atom. Therefore, the H₂ molecule is more difficult to get electrons from the MgAl1 surface. And so the dissociation energy barrier is larger on the MgAl1 surface.

IV. SUMMARY

In summary, the electronic structures of the Al-doped Mg(0001) surfaces and the dissociation behaviors of H₂ molecules on the doped surfaces are systematically studied, using the first-principles calculations. Our calculational results show that after Al-doping, the surface electronic structure is largely changed. Due to the electrons redistribution, the surface relaxation changes from expansion to contraction around the doping layer. For different doping lengths, the work function of the Mg(0001) surface are all enlarged. Through careful electronic structure analysis, we further find that the electronic states around the Fermi energy mainly distribute around the doping layer for Al-doped Mg(0001) surface. By calculating the potential energy surface of a H₂ molecule on the Al-doped Mg(0001) surfaces, we find that the doping of an Al atom does not change the dissociation path with the lowest energy barrier, but enlarges the energy barrier. And for the first layer doping, the energy barrier is changed by 0.30 eV. From wavefunction and charge-density analysis, we reveal the two interaction stages during the dissociation of the H₂ molecule, i.e. the first orthogonalization and later charge-transfer stages. We find that because more surface electrons distribute around the Al atom, the orthogonalization mainly happens between the H₂ molecule and the surface Al atom. In addition, since Al atom has a weaker ability to lose electrons, the dissociation energy barrier for H₂ is enlarged on the MgAl1 surface than on a clean Mg(0001) surface. Our studies provide a detailed mechanism for explaining the improvement on the resistance to corrosion for the Mg(0001) surface by doping of Al atoms.

Acknowledgments

P. Z. was supported by the NSFC under Grants No. 10604010 and No. 60776063. Y. W. was supported by the NSFC under Grants No. 50471070 and No. 50644041.

-
- [1] H. Fritzsche, M. Saoudi, J. Haagsma, C. Ophus, E. Lubber, C. T. Harrower, and D. Mitlin, *Appl. Phys. Lett.* **92**, 121917 (2008).
- [2] W. Grochala and P. P. Edwards, *Chem. Rev.* **104**, 1283 (2004); A. M. Seayad and D. M. Antonelli, *Adv. Mater* **16**, 765 (2004).

- [3] J. K. Nørskov, A. Houmøller, P. K. Johansson, and B. I. Lundqvist, *Phys. Rev. Lett.* **46**, 257 (1981).
- [4] P. T. Sprunger and E. W. Plummer, *Chem. Phys. Lett.*, **187**, 559 (1991).
- [5] D. M. Bird, L. J. Clarke, M. C. Payne, and I. Stich, *Chem. Phys. Lett.* **212**, 518 (1993).
- [6] T. Vegge, *Phys. Rev. B* **70**, 035412 (2004).
- [7] M. Johansson, C. W. Ostefeld, and I. Chorkendorff, *Phys. Rev. B* **74**, 193408 (2006).
- [8] G. X. Wu, J. Y. Zhang, Y. Q. Wu, Q. Li, G. Z. Zhou, and X. H. Bao, *Acta Phys. Chim. Sin.* **24**, 55 (2008).
- [9] H. Fritzsche, C. Ophus, C. T. Harrower, E. Lubner, and D. Mitlin, *Appl. Phys. Lett.* **94**, 241901 (2009).
- [10] K. U. Kainer, *Magnesium Alloys and their Applications* (WILEY-VCH Verlag GmbH, New York, 2000).
- [11] Y. F. Li, P. Zhang, B. Sun, Y. Yang, and Y. H. Wei, *J. Chem. Phys.* **131**, 034706 (2009).
- [12] Y. F. Li, Y. Yang, B. Sun, H. Z. Song, Y. H. Wei, P. Zhang, (unpublished).
- [13] G. Kresse and J. Furthmüller, *Phys. Rev. B* **54**, 11169 (1996) and references therein.
- [14] J. P. Perdew and Y. Wang, *Phys. Rev. B* **45**, 13244 (1992).
- [15] G. Kresse and D. Joubert, *Phys. Rev. B* **59**, 1758 (1999).
- [16] H. J. Monkhorst and J. D. Pack, *Phys. Rev. B* **13**, 5188 (1976).
- [17] M. Weinert and J.W. Davenport, *Phys. Rev. B* **45**, 13709 (1992).
- [18] V. Amonenko, V. Y. Ivanov, G. Tikhinskij, and V. Finkel, *Phys. Met. Metallogr.* **14**, 47 (1962).
- [19] N. W. Ashcroft and N. D. Mermin, *Solid State Physics* (Saunders, Philadelphia, 1976)
- [20] K. P. Huber and G. Herzberg, *Constants of Diatomic Molecules* (Van Nostrand, New York, 1979).
- [21] P. Staikov and T. S. Rahman, *Phys. Rev. B* **60**, 15613 (1999).
- [22] E. Wachowicz and A. Kiejna, *J. Phys.: Condens. Matter* **13**, 10767 (2001).
- [23] E. Rotenberg, J. Schaefer, and S. D. Kevan, *Phys. Rev. Lett.* **84**, 2925 (2000).
- [24] E. Sanville, S. D. Kenny, R. Smith, and G. Henkelman, *J. Comp. Chem.* **28**, 899 (2007).
- [25] P. Zhang, B. Sun, and Y. Yang, *Phys. Rev. B* **79**, 165416 (2009).
- [26] J. Harris and S. Anderson, *Phys. Rev. Lett.* **55**, 1583 (1985).
- [27] B. Hammer, K. W. Jacobsen and J. K. Nørskov, *Surf. Sci.* **297**, L68 (1993).